

JOINT INSTITUTE
FOR NUCLEAR RESEARCH

Influence of oxygen concentration on radiolytic yields and DNA damage induced by low-energy electrons

Author: Jorge Rondon Larquin

Supervisor: Dr. Ivan Padron Diaz

Abstract

DNA damage and radiolytic yields (G-values) induced by 4 keV electrons in a model cell (1 μm water sphere) were simulated using Geant4-DNA (the `dnadamage2` example). Four concentrations of dissolved oxygen (0–250 μM) were studied to cover from anoxia to normoxia under extreme conditions that would make cell survival unsustainable but justify an attempt to reproduce the dynamics of the sudden oxygen consumption during irradiation at ultra-high dose rates. G-values were obtained from the temporal evolution of reactive species up to 1 μs , and DNA damage was classified into single strand breaks (SSB) and double strand breaks (DSB) using a clustering criterion of 10 bp. The results show a strong reduction of $G(e_{\text{aq}}^-)$ with oxygen (95% at 250 μM), while the oxidizing radicals OH^\bullet , H_2O_2 and HO_2 increase gradually. These findings are consistent with the oxygen effect in radiolysis and explain the higher radiosensitivity of well-oxygenated tissues.

Contents

1	Introduction	3
1.1	Water radiolysis and indirect damage	3
1.2	Oxygen: a key modulator of radiological damage	3
1.3	Purpose of the study	3
2	Methodology	4
2.1	Simulations with Geant4-DNA and damage thresholds	4
2.2	Radiolytic yields (G-values)	5
2.3	DNA damage analysis: clustering criterion	6
3	Results	6
3.1	Temporal evolution of G-values	6
3.2	DNA damage: SSB and DSB clusters	8
4	Discussion	10
4.1	Absence of HO_2^\bullet under anoxia and its oxygen dependence	10
4.2	Influence of oxygen on hydrated electrons, oxidising radicals and ions	10
4.3	Implications for the oxygen depletion hypothesis in FLASH-RT	11
5	Conclusions	11

1 Introduction

1.1 Water radiolysis and indirect damage

When a biological system is irradiated, most of the cellular damage does not come from the direct impact of radiation on DNA but from the decomposition of surrounding water molecules. This phenomenon, known as water radiolysis, occurs because water represents about 80 % of the cellular composition. As a result of this process, highly reactive chemical species are generated, among which the hydroxyl radical (OH^\bullet), solvated electrons (e_{aq}^-), and hydrogen peroxide (H_2O_2) stand out.

The OH^\bullet radical deserves special attention because of its high oxidizing capacity, which makes it the main agent of indirect DNA damage [1]. DNA damage by radiation can occur through two pathways: the direct mechanism (direct ionization or excitation of DNA) and the indirect mechanism, mediated by free radicals that diffuse from the aqueous medium [2].

Monte Carlo track-structure simulations, such as those implemented in Geant4-DNA, allow these processes to be studied at the nanoscale, including the formation and recombination of reactive species as a function of time and dose [3].

1.2 Oxygen: a key modulator of radiological damage

Oxygen plays a determining role in radiobiology. When present during irradiation, it acts as a “fixing” agent for radical-induced damage, preventing chemical repair and making DNA lesions permanent [2]. Under hypoxia (low O_2 concentrations), as often found in solid tumours, DNA damage is reduced, thereby increasing the resistance of these cells to radiotherapy.

Conversely, under normoxia (typical O_2 concentrations in healthy tissue, about $250 \mu\text{M}$), the radicals generated by radiolysis have a higher probability of interacting with DNA and producing breaks. Thus, oxygen concentration not only affects chemical kinetics but also the efficiency of indirect damage and, ultimately, the cellular response to radiation.

1.3 Purpose of the study

From the above, a central question arises: how does oxygen concentration modify the chemical evolution of water and the DNA damage induced by low-energy electrons? Several studies have shown that low linear energy transfer (LET) radiation generates chemical species whose dynamics are very sensitive to dissolved oxygen [3].

Therefore, the present work focuses on analysing the effect of different oxygen concentrations (0, 10, 50 and 250 μM) on:

- Radiolytic yields (G-values) of the main chemical species (OH^\bullet , e_{aq}^- , H, H_2O_2)
- Analysis of single strand break (SSB) and double strand break (DSB) damage to DNA

The results are discussed in the context of the oxygen effect and its relevance for understanding the differential radiosensitivity between normoxic tissues and hypoxic tumours.

2 Methodology

2.1 Simulations with Geant4-DNA and damage thresholds

The simulations were performed with the `dnadamage2` example of Geant4-DNA, following the methodology described in [4, 3]. The radiolytic chemistry model and the Independent Reaction Times (IRT) method were implemented according to [3, 7]. The physical and chemical models of Geant4-DNA have been described in detail in the review articles [8, 9, 10], and their experimental validation is presented in [11].

A monoenergetic electron beam of 4 keV was used to irradiate a model cell (1 μm diameter water sphere). 4 keV electrons are representative of the delta electrons generated by high-energy radiation (MV photons, MeV protons), which are the main agents of DNA damage at the nanoscale. As observed in Figure 1, the track structure of these electrons is sparse and characteristic of low-LET radiation. For DNA modelling, a pUC19 plasmid of 2686 base pairs, provided by the example via the `pUC19.xyz` file, was used [4].

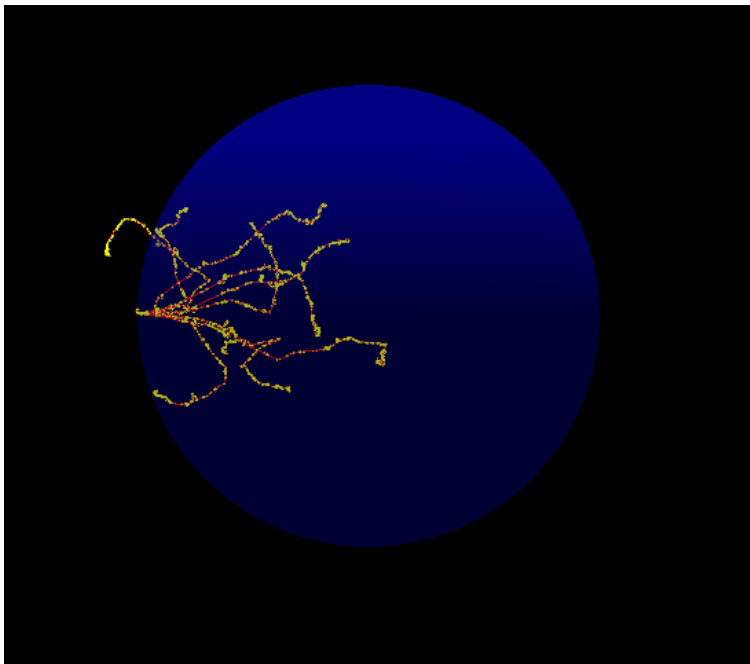


Figure 1: Trajectories of 4 keV electrons in a 1 μm diameter water sphere. A sparse track structure is observed, with isolated ionisation events, characteristic of low linear energy transfer (LET) radiation.

To simulate the chemical evolution, the Independent Reaction Times (IRT) method was used. It approximates the kinetics by stochastic events, calculating a potential time for each possible reaction between pairs of molecules based on their distance and diffusion coefficients, drastically reducing the computational cost compared to step-by-step (SBS) methods while maintaining a precision $>90\%$ in predicting DNA damage [7]. The chemical time was set to 1 μs , sufficient to capture the formation, diffusion and recombination of primary reactive species. The time step for chemical integration was set to 1 ps, the default value of the `dnadamage2` example.

2.2 Radiolytic yields (G-values)

Radiolytic yields quantify the number of species produced or consumed per 100 eV of absorbed energy. Their expression is given by:

$$G = \frac{N \cdot 100}{E} \quad (1)$$

where:

- G : number of molecules of a chemical species produced per 100 eV of absorbed energy.

- N : total number of molecules of that species.
- E : total energy absorbed by the medium (in eV).

2.3 DNA damage analysis: clustering criterion

To quantify double strand breaks (DSB), a clustering method based on the following steps was implemented:

1. **Spatial grouping:** Single strand breaks (SSB) are grouped into *clusters* when their positions in the DNA sequence are ≤ 10 base pairs (bp) apart. This threshold corresponds approximately to one turn of the DNA helix (3.4 nm) and is the standard value used in DNA damage simulations [13, 5].
2. **Strand verification:** Once the clusters are formed, the presence of at least one break on each of the two strands within each cluster is examined.
3. **DSB counting:** If a cluster contains breaks on both strands, a single DSB is counted. This criterion avoids the overestimation characteristic of pairwise methods, which would count every possible combination of breaks on opposite strands as independent DSBs.

This approach has been widely validated in the literature for the study of low-LET radiation damage [13, 4], and is consistent with the biological definition of complex damage, where the spatial proximity of lesions on both strands hinders their repair [6].

The energy threshold for considering an SSB was set to 17.5 eV, the standard value in Geant4-DNA for the sugar-phosphate bond break [12], supported by validation studies [13].

3 Results

3.1 Temporal evolution of G-values

Figure 2 shows the radiolytic yields of the main species for times from 1 ps to 1 μ s, for the four simulated oxygen concentrations (0, 10, 50 and 250 μ M).

In the absence of dissolved oxygen (0 μ M), no significant formation of the hydroperoxyl radical (HO_2^\bullet) was observed. However, as the concentration increases, the production of this species increases.

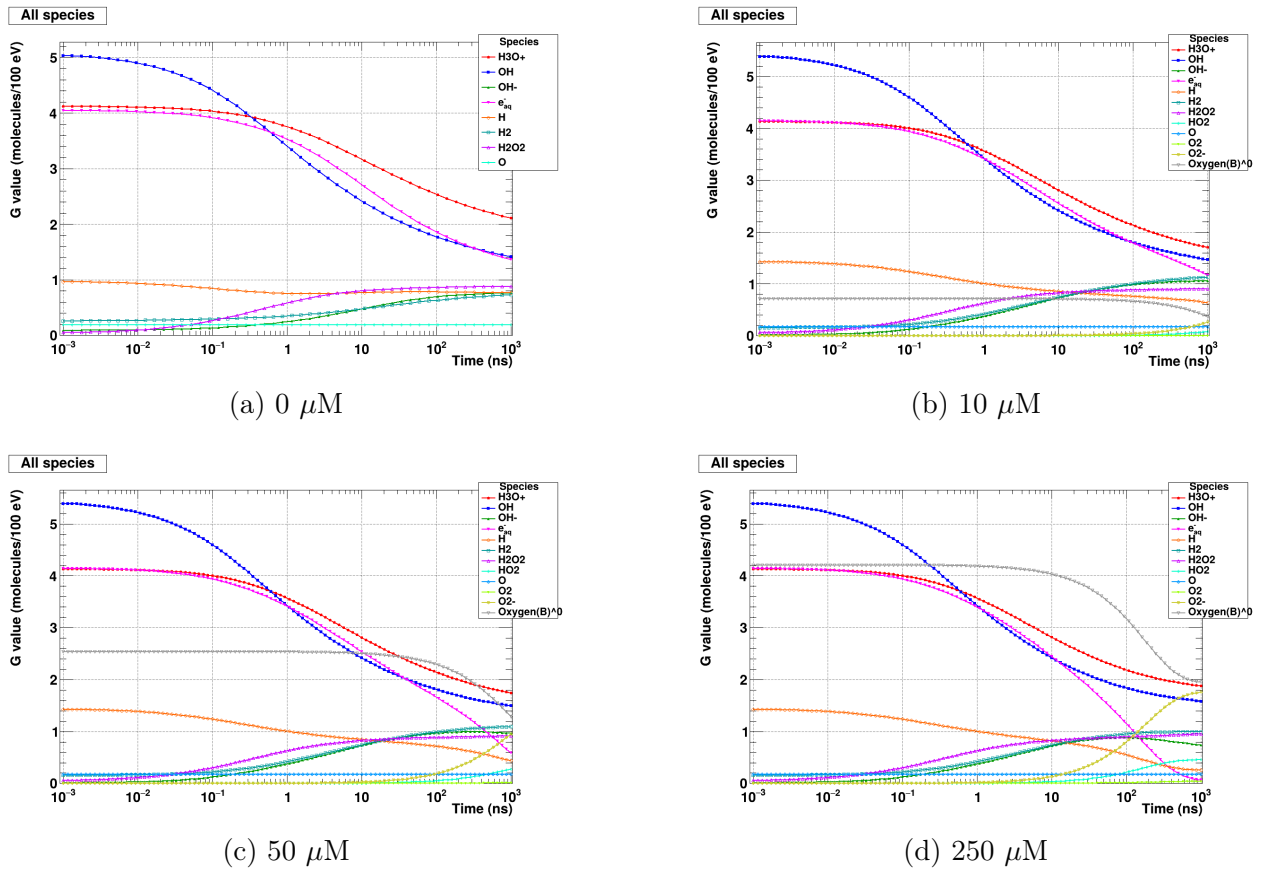


Figure 2: Behaviour of radiolytic yields (G-values) as a function of oxygen concentration.

It is common for all four cases that the dominant species at early times are H_3O^+ , OH^\bullet and e_{aq}^- , which are the final products of the physico-chemical stage occurring between 1 and 100 ps. A monotonic decrease is observed for longer times up to $1 \mu\text{s}$. Table 1 shows the relative changes of the three species, where the hydrated electron at $1 \mu\text{s}$ is seen to be reduced almost completely.

Table 1: Relative change of G-values at 1 μs with respect to the initial oxygen concentration.

Species	[O ₂] (μM)	G-value	Absolute ΔG	ΔG (%)
H ₂ O ₂	0	0.884	0.000	0.0
	10	0.906	0.023	2.6
	50	0.919	0.035	4.0
	250	0.956	0.072	8.1
OH [•]	0	1.418	0.000	0.0
	10	1.467	0.049	3.5
	50	1.498	0.080	5.6
	250	1.583	0.165	11.6
e _{aq} ⁻	0	1.363	0.000	0.0
	10	1.167	-0.196	-14.4
	50	0.584	-0.779	-57.1
	250	0.068	-1.294	-95.0

A strong dependence of $G(e_{\text{aq}}^-)$ on oxygen concentration is observed, where increasing the concentration produces a significant reduction of hydrated electrons at 1 μs (Figure 3).

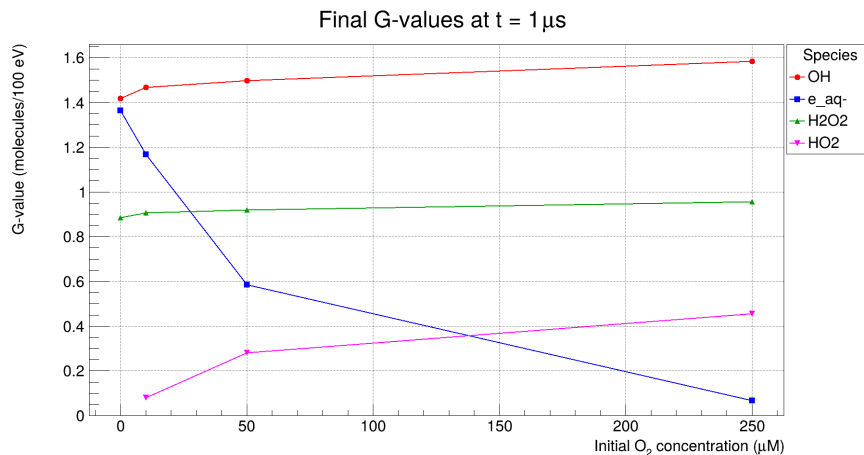


Figure 3: G-values as a function of oxygen concentration at 1 μs .

3.2 DNA damage: SSB and DSB clusters

Table 2 summarises the DNA damage as a function of oxygen concentration. It includes the total number of single strand breaks (SSB), the number of double strand break (DSB)

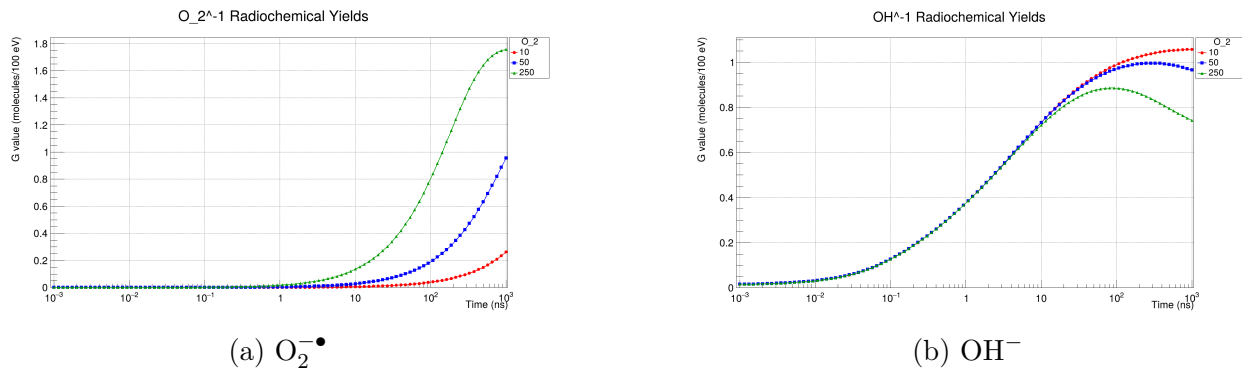


Figure 4: Radiolytic yields (G-values) for superoxide anion (a) and hydroxyl ion (b) as a function of oxygen concentration.

clusters obtained using a 10 bp clustering criterion, and the DSB/SSB ratio expressed as a percentage.

Table 2: DNA damage as a function of oxygen concentration.

O_2 concentration (μM)	Total SSB	DSB	DSB/SSB (%)
0	1907	10	0.5
10	1844	13	0.7
50	1633	15	0.9
250	1766	19	1.1

It is observed that the number of SSB reaches a maximum at low concentrations (0-10 μM) and then decreases slightly, while DSB gradually increase with oxygen concentration, rising from 13 to 19 between 0 and 250 μM . Consequently, the DSB/SSB ratio increases from 0.7% to 1.1%, indicating that a higher availability of O_2 not only increases total damage but also favours the formation of more complex and lethal lesions (DSB).

Correlation between radiolytic yields and DNA damage To quantify the relationship between reactive species and DNA damage, the Pearson correlation coefficient was calculated between the G-values at 1 μs (Table 1) and the DSB/SSB ratio (Table 2). The results are summarised in Table 3.

A nearly perfect correlation was obtained for the OH^{\bullet} radical ($r = 0.95$) and for H_2O_2 ($r = 0.95$), confirming that both oxidising species are directly associated with the increase in lethal DNA damage. In contrast, the hydrated electron showed a strong negative correlation ($r = -0.99$), indicating that its decrease in the presence of oxygen removes an important radical recombination pathway, thereby enhancing damage. These results are consistent with

Table 3: Pearson correlation coefficients (r) between G-values and DSB/SSB.

Species	Correlation coefficient r
OH \bullet	0.9517
H ₂ O ₂	0.9488
e _{aq} ⁻	-0.9883

the oxygen effect and quantitatively validate the cause-effect relationship between radiolytic yields and the complexity of DNA damage.

4 Discussion

4.1 Absence of HO₂ \bullet under anoxia and its oxygen dependence

The fact that G(HO₂ \bullet) is zero at 0 μ M is because its production depends directly on O₂, either via the reaction H \bullet + O₂ \rightarrow HO₂ \bullet or through protonation of the superoxide anion (O₂ \bullet^- + H⁺ \rightleftharpoons HO₂ \bullet), which itself is generated from molecular oxygen. Therefore, under anoxic conditions, the yield of HO₂ is practically zero. This situation changes gradually as the oxygen concentration increases.

4.2 Influence of oxygen on hydrated electrons, oxidising radicals and ions

Capture of hydrated electrons and increase of superoxide anion The behaviour of hydrated electrons is due to the capture reaction of the hydrated electron by molecular oxygen ($e_{\text{aq}}^- + \text{O}_2 \rightarrow \text{O}_2^{\bullet-}$), which competes with other recombination processes. This results in an increase of G(O₂ \bullet^-) with oxygen concentration.

Increase of oxidising radicals and decrease of ions In contrast, the species OH \bullet , H₂O₂ and HO₂ show a gradual increase with O₂ concentration. This increase reflects that oxygen, by removing hydrated electrons and hydrogen radicals, reduces the recombination pathways that consume oxidising radicals, thereby increasing their final yields and reducing species such as OH⁻ and HO₂⁻ as the dissolved oxygen concentration increases, which are products of these reactions. Figure 4 shows the behaviour of both O₂ \bullet^- and OH⁻, which corroborates the above. These results are consistent with the oxygen effect in radiolysis, where O₂ acts as a sensitiser by fixing radical damage and modulating the kinetics of reactive species.

4.3 Implications for the oxygen depletion hypothesis in FLASH-RT

The findings of this work support the oxygen depletion hypothesis in FLASH radiotherapy. The rapid drop in O_2 concentration during ultra-high dose rate irradiation would induce a transient hypoxia that, according to our results, reduces the production of oxidising radicals (OH^\bullet , H_2O_2 , HO_2) and increases the survival of hydrated electrons, modifying radical recombination and decreasing DNA damage in healthy tissue. The quantitative correlation between G-values and DSB/SSB observed in this work supports this mechanism.

5 Conclusions

In this work, the effect of oxygen concentration on water radiolysis and DNA damage induced by 4 keV electrons was investigated using Monte Carlo simulations with Geant4-DNA (the `dnadamage2` example). A clear dependence of radiolytic yields and strand breaks on dissolved oxygen concentration was observed.

The hydrated electron (e_{aq}^-) was found to be highly sensitive to O_2 concentration, with a 95% reduction in its yield when going from anoxic to normoxic conditions (250 μ M). In contrast, the oxidising radicals OH^\bullet , H_2O_2 and HO_2 gradually increase with oxygen concentration, reflecting the role of O_2 as an electron scavenger and modulator of recombination pathways. DNA damage, quantified by single strand breaks (SSB) and double strand breaks (DSB), showed an almost perfect correlation with the yields of oxidising species ($r > 0.95$), while the correlation was strongly negative for the hydrated electron ($r = -0.99$). The DSB/SSB ratio increased from 0.7% under anoxia to 1.1% under normoxia, indicating that oxygen not only increases total damage but also its complexity.

As future work, it is proposed to extend this study by incorporating the dynamic kinetics of oxygen consumption during irradiation, as well as simulation under ultra-high dose rate (FLASH-RT) conditions. This would allow evaluating how transient oxygen depletion modifies radiolytic yields and DNA damage, and directly comparing conventional and FLASH regimes for different initial O_2 concentrations. Taken together, these findings provide a quantitative basis for understanding the oxygen effect and its potential exploitation in FLASH radiotherapy.

References

- [1] LaVerne, J. A. (2000). OH radicals and oxidizing products in the radiolysis of water. *Journal of Physical Chemistry B*, 104(40), 10288–10294.
- [2] Spitz DR, Buettner GR, Petronek MS, et al. An integrated physico-chemical approach for explaining the differential impact of FLASH versus conventional dose rate irradiation on cancer and normal tissue responses. *Radiother Oncol.* 2019;139:23-27.
- [3] Ramos-Méndez J, Domínguez-Kondo N, Schuemann J, McNamara A, Moreno-Barbosa E, Faddegon B. LET-dependent intertrack yields in proton irradiation at ultra-high dose rates relevant for FLASH therapy. *Radiat Res.* 2020;194(4):351-362. doi:10.1667/RADE-20-00084.1.
- [4] D-Kondo JN, Moreno-Barbosa E, Štěpán V, et al. DNA damage modeled with Geant4-DNA: effects of plasmid DNA conformation and experimental conditions. *Phys Med Biol.* 2021;66(24):245017. doi:10.1088/1361-6560/ac3a22.
- [5] Matsuya Y, Kai T, Yoshii Y, et al. Modeling of yield estimation for DNA strand breaks based on Monte Carlo simulations of electron track structure in liquid water. *J Appl Phys.* 2019;126:124701. doi:10.1063/1.5115519.
- [6] Baatout S (ed). *Radiobiology Textbook*. Springer; 2023. doi:10.1007/978-3-031-18810-7.
- [7] Karamitros M, Luan S, Bernal MA, et al. Diffusion-controlled reactions modeling in Geant4-DNA. *J Comput Phys.* 2014;274:841-882.
- [8] Bernal MA, Bordage MC, Brown JMC, et al. Track structure modeling in liquid water: A review of the Geant4-DNA very low energy extension of the Geant4 Monte Carlo simulation toolkit. *Phys Med.* 2015;31(8):861-874. doi:10.1016/j.ejmp.2015.10.087.
- [9] Incerti S, Kyriakou I, Bernal MA, et al. Geant4-DNA example applications for track structure simulations in liquid water: A report from the Geant4-DNA Project. *Med Phys.* 2018;45(11):e722-e739. doi:10.1002/mp.13048.
- [10] Incerti S, Kyriakou I, Bernal MA, et al. Review of chemical models and applications in Geant4-DNA: Report from the ESA BioRad III Project. *J Appl Phys.* 2019;125(10):104301. doi:10.1063/1.5087891.
- [11] Incerti S, Ivanchenko A, Karamitros M, et al. Comparison of Geant4 very low energy cross section models with experimental data in water. *Med Phys.* 2010;37(9):4692-4708. doi:10.1118/1.3476457.

- [12] Incerti S, Baldacchino G, Bernal M, et al. The Geant4-DNA project. *Int J Model Simul Sci Comput.* 2010;1(2):157-178. doi:10.1142/S1793962310000222.
- [13] Chatzipapas KP, Papadimitroulas P, Obeidat M, et al. Quantification of DNA double-strand breaks using Geant4-DNA. *Med Phys.* 2019;46(1):405-413. doi:10.1002/mp.13290.